IEEE Access
Multidisciplinary | Rapid Review | Open Access Journal

Received 23 March 2023, accepted 11 April 2023, date of publication 14 April 2023, date of current version 21 April 2023.

Digital Object Identifier 10.1109/ACCESS.2023.3267389

RESEARCH ARTICLE

A Novel Method of Vector Shift Criterion Utilization in Power System Automation

KAROL SWIERCZYNSKI, MARCIN HABRYCH, AND BARTOSZ BRUSILOWICZ, (Senior Member, IEEE)
Faculty of Electrical Engineering, Wroclaw University of Science and Technology, 50-370 Wroclaw, Poland
Corresponding author: Bartosz Brusilowicz (bartosz.brusilowicz@pwr.edu.pl)

ABSTRACT The article describes the new application of a well-known protection criterion - Vector Shift (VS). In the paper, technical problems related to the utilization of this criterion have been described. Additionally, the authors conducted laboratory tests of a digital protection relay. The impact of different disturbances occurring in the power systems on the operation of the Vector Shift criterion has been examined. The obtained results have proved the validity of banning the Vector Shift criterion in some countries. Furthermore, a novel application of the Vector Shift criterion has been presented. This criterion could be utilized to determine the degree of balance of a separated island. This information may be helpful in novel power system protection devices used in Smart Grids or microgrids.

INDEX TERMS Vector Shift, power system protection, island operation, distributed generation, smart grids, microgrids.

I. INTRODUCTION

Vector Shift is a well-known and, in the past, commonly used island detection criterion [1], [2]. The working principle of the Vector Shift criterion is to detect a step change in the phase angle between the voltage vectors of the distributed generation and the power system [3], [4], [5], [6], [7]. This change accompanies the separation of the uncontrolled island. If the measured value of the voltage phase angle change exceeds a preset threshold, the generating unit is switched off. The Vector Shift algorithm implementation method is proposed in [8].

There are several problems related to the operation of the Vector Shift criterion. The first issue is related to the non-detection zone (NDZ) [9]. During islanding with a relatively accurate power balance, the VS relays may have problems with detecting this phenomenon. The detection time may increase; therefore, the safe operation of the grid decreases. Moreover, in the condition of perfect power balance, islanding cannot be detected [5], [10]. In [11], [12], and [13], the research related to the accuracy of island detection in different active and reactive power balance scenarios is presented. The authors proved that the tripping time of the VS relay decreases according to increasing active power imbalance.

Furthermore, the Vector Shift criterion is characterized by sensitivity to different system-wide disturbances [10], [14], [15]. This problem negatively affects the operation of this algorithm and may even lead to undesirable misoperations. The literature describes real cases of power system disruptions misinterpreted by the Vector Shift criterion. An example of such an event is the shutdown of distributed generation of about 400 MW in 2016 in the United Kingdom [16].

Another problematic aspect related to the operation of the Vector Shift criterion is the appropriate selection of setting groups. In this process, a compromise must be reached. Too much sensitivity could result in unnecessary shutdowns during external disturbances. On the other hand, underestimating sensitivity may result in a lack of tripping in the case of isolation of the island [16]. The authors conducted laboratory tests to determine the impact of settings and the occurrence of disturbances in the power system on the operation of the Vector Shift criterion. The conclusions of these tests are presented in the following sections.

Besides, the authors of [5], [6], [17], [18], [19], [20], and [21] conducted comprehensive research related to different features and properties of the Vector Shift relays. Both

The associate editor coordinating the review of this manuscript and approving it for publication was Akshay Kumar Saha.

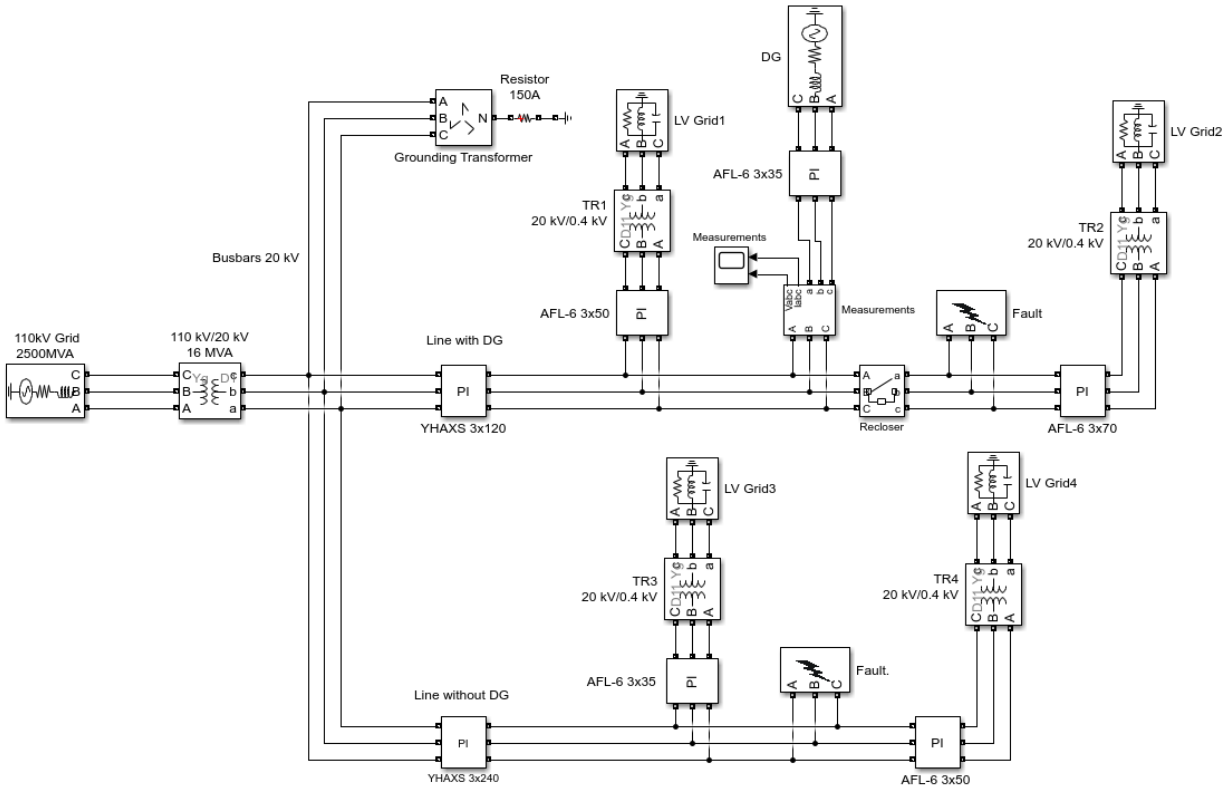

FIGURE 1. The MV grid model with distributed generation.

tripping time and operation effectiveness were investigated. During the tests, the impact of various parameters was examined. Not only the power imbalance was changed, but also generator inertia, parameters of feeders, and fault types and conditions. Analyzing the results, it can be concluded that in certain cases, VS criterion operates incorrectly.

The authors of this article conducted equally complex and detailed tests. However, they have focused on different aspects. The cited papers concern mainly the properties of the Vector Shift algorithm related to power system protection. Hitherto this criterion was utilized to island detection. The authors of this article propose a new approach to the utilization of the Vector Shift criterion. They show that by measuring the sign of phase shift, accompanied islanding process of distributed generation, significant information might be obtained. This information could be utilized both in regulatory processes and power system protection devices. The examined issue is a novelty.

II. THE IMPACT OF EXTERNAL DISTURBANCES ON VECTOR SHIFT CRITERION OPERATION

The digital relay with implemented Vector Shift algorithm has been examined. Different states and types of faults have been simulated to determine the immunity to external disturbances. Especially 1-phase earth faults were simulated because they are the most common disturbance in medium voltage grids. The COMTRADE files with disturbance voltage time waveforms have been obtained using the MV grid model with distributed generation (DG) created in the MATLAB-Simulink software (Fig.1). The model is based on real parameters of the real MV grid in Poland. The first part of the model consists of a fragment of the 110 kV grid, a 110/20 kV transformer, and a grounding transformer connected to the 20 kV bus bars. The modeled MV grid operates as ineffectively grounded, with the artificial neutral point grounded through a resistor. Afterward, the two medium-voltage lines were also modeled. The 20/0.4 kV stations representing consumers were connected to the lines. Both lines are equipped with blocks that allow the simulation of different types of faults. In the line with distributed generation (DG), faults are simulated in the section downstream of the point of common coupling (PCC). This allows assuming that the disturbance occurring in this part of the line should be eliminated by the recloser with protection. Therefore, the fault should not adversely affect the operation of the distributed generation. Whereas the faults occurring in the line without DG should not have any impact on the stable operation of the generating unit. The parameters of the MV grid model are presented in Table 1.

Utilizing the developed model, simulations including different types of faults were conducted, and the COMTRADE files were generated. The COMTRADE files contained waveforms of voltages and currents from the measurement block (Fig. 1). Then, using Omicron CMC356 tester, and generated COMTRADE files protection relay has been examined (Fig.2). The standard setting range of the Vector Shift

TABLE 1. Parameters of medium voltage grid.

Element	Quantity	Value
110 kV Grid	Short-circuit level	2500 MVA
110 kV/20 kV transformer	Nominal power	16 MVA
20 kV/0.4 kV transformer	Nominal power	0.1 MVA
LV load	Nominal power	0.08 MVA
240 mm^2 cable line	Length	80 m
120 mm^2 cable line	Length	500 m
70 mm^2 overhead line	Length	500 m
50 mm^2 overhead line	Length	550 m
35 mm2 overhead line	Length	50 m

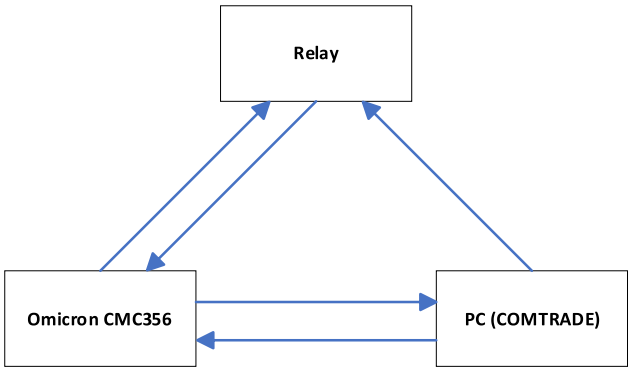

FIGURE 2. The flowchart of the laboratory layout.

criterion, according to the application notes of individual manufacturers and [16], is from 6 to 12 degrees. Therefore, during the tests, the settings, fault location, fault resistance, and fault type were changed.

In the case of 1-phase earth faults in the line without distributed generation, the number of tripping has depended on setting and fault resistance. Table 2 presents the statistical results of the tests in the case of a settings group from the 6 to 10 degrees range. While Table 3 includes results for the setting group from the 10 to 12 degrees range.

It can be concluded that the utilization of settings from the lower range negatively affects the selectivity of operation. External disturbances cause undesirable trippings in 100% of examined cases. However, increasing of setting improves the operation of the relay.

Figure 3 presents the example of simulated voltage-time waveforms during 100 Ω 1-phase fault in the line without distributed generation (Fig. 1). To better illustrate the simulated disturbance, the vector graphs of three-phase voltages,

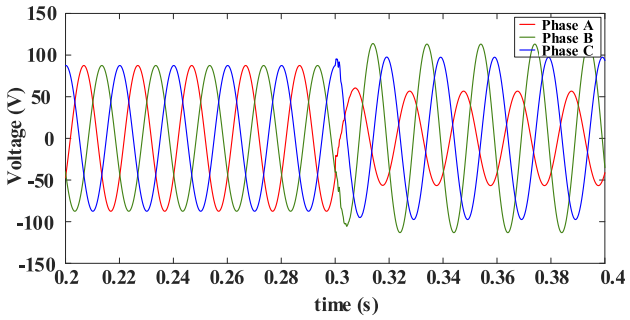

FIGURE 3. The voltage-time waveform during 100 Ω 1-phase fault.

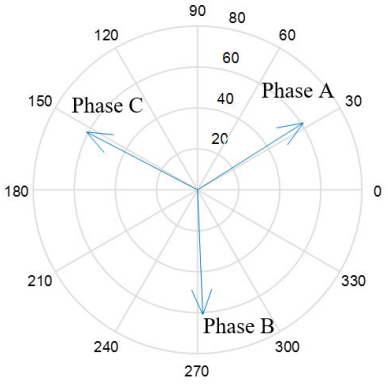

FIGURE 4. The vector graphs of voltages before the 100 Ω 1-phase fault.

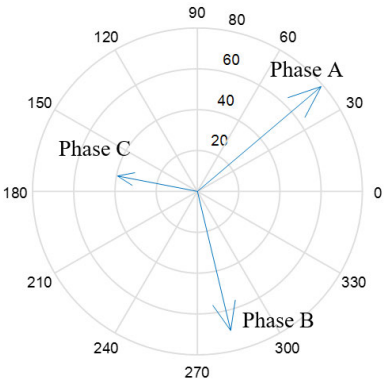

FIGURE 5. The vector graphs of voltages before the 100 Ω 1-phase fault.

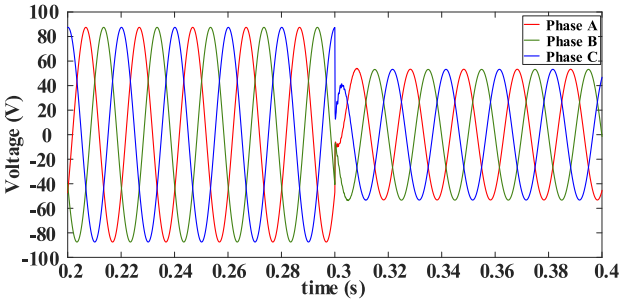

FIGURE 6. The voltage-time waveform 10 Ω 3-phase fault.

for the same case, before and during the fault are presented in Figures 4 and 5.

TABLE 2. Shutdown statistics for settings from the 6 to 10 degrees range.

Fault type	Fault location	Fault resistance	Percentage of false tripping
1-phase	Line without DG	100 Ω	100 %
1-phase	Line without DG	50 Ω	100 %
1-phase	Line with DG	100 Ω	100 %
1-phase	Line with DG	50 Ω	100 %
3-phase	Line with DG	10 Ω	100 %
3-phase	Line without DG	10 Ω	100 %

TABLE 3. Shutdown statistics for settings from the 10 to 12 degrees range.

Fault type	Fault location	Fault resistance	Percentage of false tripping
1-phase	Line without DG	100 Ω	0 %
1-phase	Line without DG	50 Ω	100 %
1-phase	Line with DG	100 Ω	0 %
1-phase	Line with DG	50 Ω	100 %
3-phase	Line with DG	10 Ω	100 %
3-phase	Line without DG	10 Ω	0 %

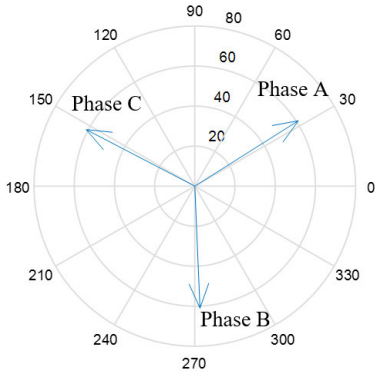

FIGURE 7. The vector graphs of voltages before the 10 Ω 3-phase fault.

The example of an instance of a 10 Ω 3-phase fault that was simulated in the line with distributed generation (Fig.1) is presented in Figure 6. Furthermore, the disturbance is also presented using vector graphs of voltages before and during the fault (Figures 7 and 8).

The results of the laboratory tests of the relay are summarized in Tables 2 and 3. The use of the low settings of the VS element caused misoperations for all tested cases regardless of the fault resistance and the location (Tab. 1). For higher settings (Tab. 2), in some cases, the relay operated correctly. In the case of the 1-phase faults, fault resistance was the most crucial factor. In the case of 3-phase faults, the negative impact on the operation of the Vector Shift criterion is related to the fault location. As can be seen, only faults in the line with distributed generation cause misoperations.

The performed laboratory tests using the protection relay show that the operation of the VS criterion may be affected by other disturbances. Due to the high probability of misoperations that can occur during events unrelated to islanding, in some countries, the Vector Shift is no longer used in island detection. This criterion has been replaced by other algorithms, usually ROCOF [22], [23], [24], [25], [26], [27].

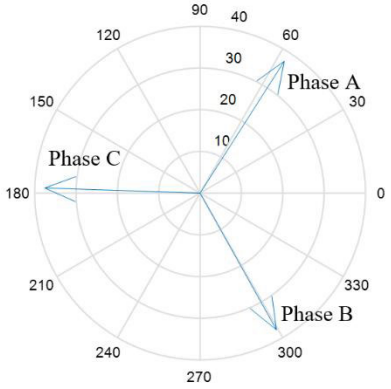

FIGURE 8. The vector graphs of voltages before the 10 Ω 3-phase fault.

III. VECTOR SHIFT ALGORITHM

In previous sections, the utilization of the Vector Shift criterion in power system protection is described. However, the authors of this paper would like to focus on the aspect related to power system automation. Comprehensive research has been conducted to examine the suitability of the Vector Shift for control and regulation processes. Firstly, using MATLAB/Simulink, the Vector Shift algorithm was developed. A simplified flowchart of this algorithm is presented in Figure 9. The proposed algorithm is implemented in the same form separately for each phase.

The first step of the algorithm is a measurement of the first harmonic of input phase voltage. The second block is the calculation of the wavelength. There are several methods to calculate the cycle. Nevertheless, the authors used a well-known algorithm - zero crossing detection with a correction. In the algorithm, sample by sample, the sign of the signal sample is determined. Based on this, the number of samples in half-periods is calculated. Depending on the sign of successive samples, appropriate calculations are executed using equations (1)–(4). In the equations, $s_x(n)$ is the sample of the measured signal for phases $x = \mathrm{A}, \mathrm{B}, \mathrm{C}$, and n is the sample number.

$$\begin{aligned} &s_x\,(n-1) > 0\ \&\ s_x\,(n) > 0; \\ &\qquad b_x = 0;\ a_x = a_x + 1; \end{aligned} \tag{1}$$

$$\begin{aligned} &s_x\,(n-1) < 0\ \&\ s_x\,(n) < 0; \\ &\qquad a_x = 0;\ b_x = b_x + 1; \end{aligned} \tag{2}$$

$$\begin{aligned} &s_x\,(n-1) < 0\ \&\ s_x\,(n) > 0; \\ &\qquad c_{1x} = s_x(n)/(s_x(n) - s_x(n-1)); \\ &\qquad m_{05x} = b_x + 1 - c_{1x} + c_{2x} \end{aligned} \tag{3}$$

$$\begin{aligned} &s_x\,(n-1) > 0\ \&\ s_x\,(n) < 0; \\ &\qquad c_{2x} = s_x(n)/(s_x(n) - s_x(n-1)); \\ &\qquad m_{05x} = a_x + 1 - c_{2x} + c_{1x} \end{aligned} \tag{4}$$

The signs of consecutive samples are compared. In the case the signs are equal, the current total of samples in half-period - a_x, b_x - is increased. These values are incremented sample by sample. Whereas in the case the signal crosses

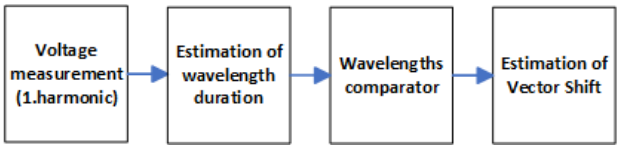

FIGURE 9. The flowchart of the Vector Shift algorithm.

zero, the corrective coefficients c_{1x} and c_{2x}, for positive and negative half-period, are calculated, respectively. Afterward, using obtained quantities, and depending on the sign of half-period, the total of samples in half-period after correction – m_{05x} – is calculated. In the next step, the duration of a given half-period - $t_x(m)$ - is estimated (5), where m is the number of half-period, and f_s is sample frequency.

$$t_x\,(m) = m_{05x}/0.5f_s \tag{5}$$

Based on the calculated value of half-period t_x, the difference between the current - $T_x(m)$ and previous - $T_x(m-1)$ duration of the period of the input signal is calculated. Then, the obtained difference is utilized for the estimation of the final value of the Vector Shift (VS_x) using (6).

$$\mathrm{VS}_x = \frac{(T_x\,(m-1) - T_x(m)) * 360^\circ}{T_x(m-1)} \tag{6}$$

Moreover, the important aspect is phase shift detection of the change occurring nearby zero-crossing of the measured voltage. In this case, both the current and the previous half-period would have different numbers of samples. As a consequence, the duration of these half-periods would be different from the nominal value. This phenomenon is presented in Figure 10.

For this reason, in the developed Vector Shift algorithm, full-period averaging is utilized. Hence, the obtained phase shift value corresponds to the actual change in voltage angle.

The developed algorithm was used in further computer simulations related to island balancing. The methodology and the results of these simulations are described in section IV.

IV. ISLAND BALANCING

Despite difficulties in the Vector Shift utilization, this criterion has other interesting properties. These features could be utilized to determine the degree of balance of a separate island. In this part of the paper, the authors would like to present their research on novel Vector Shift utilization methods.

A simplified model of a double-feed medium voltage grid has been developed to examine the operation of the Vector Shift criterion thoroughly. This model is presented in Figure 11. The model contains two sources of electricity, the power system on the one side and the distributed generation on the other side. The loads are connected to the grid on both sides of the model. Furthermore, the beginning and the end are equipped with voltage, current, and vector shift measurements. Using this information in the point of common coupling (PCC), the transfer of active and reactive power can be calculated. The breaker is installed in the PCC. Therefore,

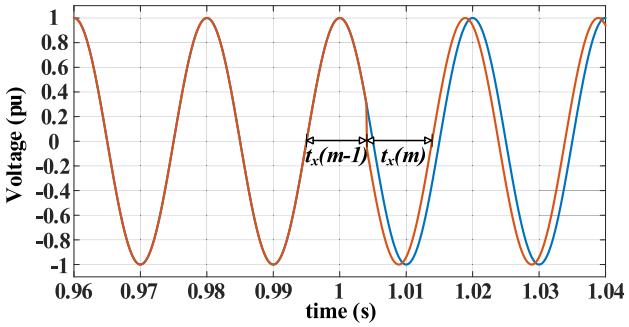

FIGURE 10. The simplified double-feed MV grid model.

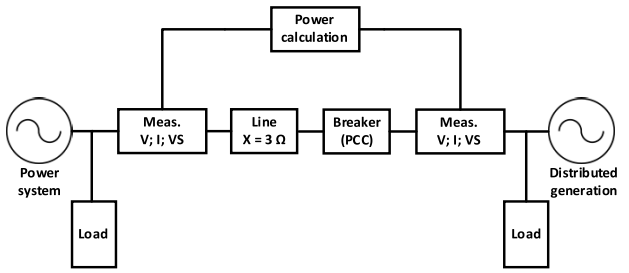

FIGURE 11. The simplified double-feed MV grid model.

different MV grid operation types, such as islanding, can be simulated.

Different scenarios of the Vector Shift criterion operation were examined during the tests. To properly modeling of the power system and distributed generation, their 3-phase short-circuit levels were set to 2500 MVA and 15 MVA, respectively. The sources are connected through the line model, with an impedance of 3 Ω. Furthermore, the power flow direction was modified by changing distributed generation's phase angle in the range between 0 and 30 degrees. Based on this information, the simulations in the MATLAB Simulink program were conducted. Consequently, the values of active and reactive power flow were calculated using formulas (7) and (8), respectively [28].

$$P = \frac{EV}{X} sin\delta \tag{7}$$

$$Q = \frac{EV}{X} cos\delta - \frac{V^2}{X} \tag{8}$$

where: E – voltage at the beginning of the line, V – voltage at the end of the line, δ – a difference of angles between E and V, X – line reactance.

Moreover, further simulations were performed to determine the value and the sign of phase shift during islanding. In this part of the simulations, the power flow was also modified by phase angle changes. Additionally, the load power has also been changed, in the range of 1 to 4 MW. During simulations, the breaker at the point of common coupling was switched on and off, accordingly to the simulated scenario. The partial results of the simulations are presented in Table 4. In this case, the load power has a value of 2 MW.

TABLE 4. Degree of balance of a separated is land.

Rate of balance	Percentage of balance	Vector Shift
power shortage	85 %	-7,26 °
	86 %	-6,84 °
	87 %	-6,43 °
	88 %	-6,01 °
	89 %	-5,18 °
	90 %	-4,77 °
	91 %	-4,35 °
	92 %	-3,93 °
	93 %	-3,10 °
	94 %	-2,69 °
	95 %	-2,27 °
	96 %	-1,44 °
	97 %	-1,02 °
	98 %	-0,61 °
	99 %	-0,19 °
balance	100 %	0,64 °
	101 %	1,06 °
	102 %	1,48 °
	103 %	2,31 °
	104 %	2,73 °
	105 %	3,15 °
power excess	106 %	3,98 °
	107 %	4,40 °
	108 %	4,82 °
	109 %	5,65 °
	110 %	6,07 °
	111 %	6,49 °
	112 %	7,33 °
	113 %	7,75 °
	114 %	8,59 °
	115 %	9,01 °

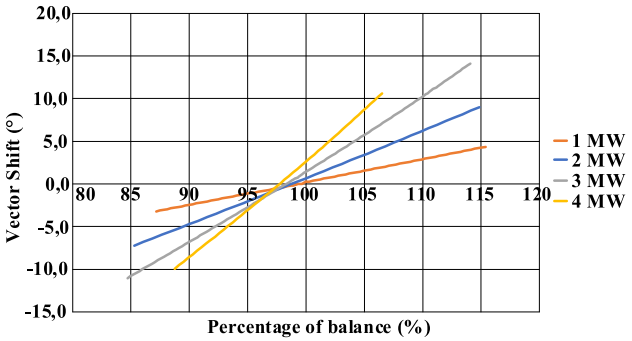

FIGURE 12. The impact of the rate of balance on the vector shift in different scenarios.

As can be seen, the value and the sign of the vector shift depend on the island's balance rate. In the case where most of the load power is covered by the power system, the sign of the vector shift during islanding is negative. Whereas the distributed generation provides most of the load power, the sign is positive. In the case of balance between the power system and the distributed generation, the value of Vector Shift is the least and oscillates around zero.

Figure 12 presents the comprehensive results of conducted tests. It contains different simulation scenarios with varied power flow directions and load power. As can be seen, the increase in load power is accompanied by an increase in the

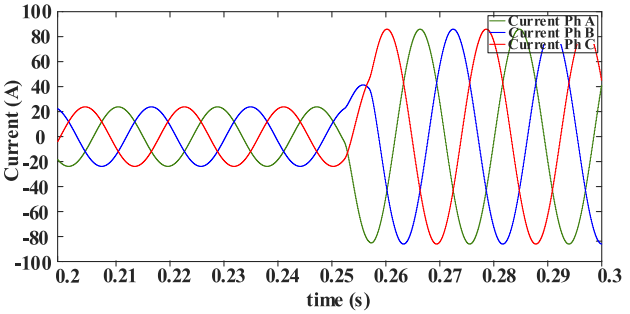

FIGURE 13. The current-time waveforms in the case of 85% power imbalance.

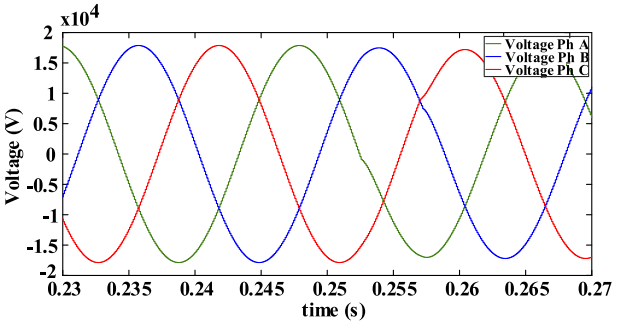

FIGURE 14. The voltage-time waveforms in the case of 85% power imbalance.

inclination of the line. In consequence, the values of Vector Shift are higher.

Another interesting conclusion drawn by conducted tests is voltage- and current-time waveforms during islanding. The boundary cases, where the power imbalance has the highest and the lowest value, were analyzed. The time waveforms are presented in Figures 13-16. It can be concluded that in dependence on the percentage of the island's balance, voltage and current waveforms shift in relation to each other. The value of this shift is defined by a Vector Shift value (Table 4). Furthermore, the RMS values of the current are different.

To conclude, the Vector Shift sign information may be helpful in power system management. The proposed methods of utilization are described in the next section.

V. POTENTIAL APPLICATIONS

The utilization of the Vector Shift criterion may not be limited to only protective functions. As mentioned previously, the sign and the value of vector shift can be valuable information. The first potential application of this algorithm is load control. By identifying the degree of balancing of the island, it is possible to determine whether distributed generation covers the power demand. In the case of the failure and isolation of the part of the grid with distributed generation, the island's load power could be controlled. Therefore, the nominal value of the frequency could be kept. The parameters of the electrical power quality would be maintained. Hence, the isolated island might operate until failure removal. The consumers would not be affected by the outage. This application can be defined as a load-shedding algorithm.

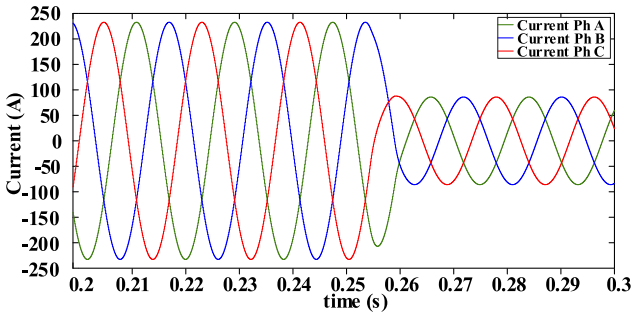

FIGURE 15. The current-time waveforms in the case of 115% power imbalance.

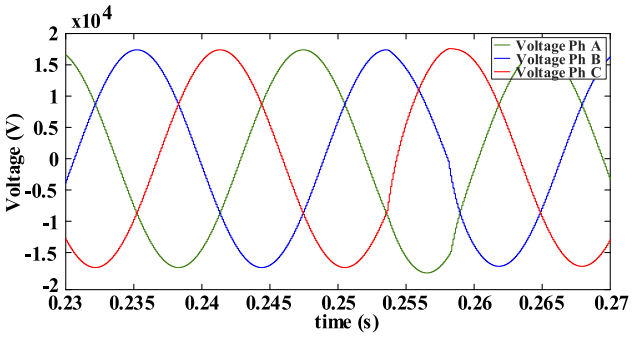

FIGURE 16. The voltage-time waveforms in the case of 115% power imbalance.

Nevertheless, the sign and the value of vector shift could be utilized in another controlling process. In this application, the controlled parameter would be the production of electricity. Similarly, as in the previous case, the information gained during islanding would be utilized to keep the nominal value of the frequency. However, in this method, the generated power would be varied. To optimize the control process, battery energy storage systems (BESS) must be utilized. BESS would be recharged, while the generated power excess would stabilize the power balance during unfavorable moments.

The control process might be improved by utilizing both described methods. Therefore, renewable energy sources could be utilized optimally. Consequently, this will positively affect the natural environment.

Furthermore, the information regarding the sign and the value of the vector shift could be helpful during the transition of the microgrid from the grid to the island operation. According to [29], this transition might be performed either as seamless or as a black start. In both methods, the distributed generation installed in the microgrid, such as PV, wind turbines, or BESS, could be controlled optimally to achieve nominal parameters possibly soon. The authors of [30] described a black start in specific conditions with a single PV with the generating power equal to load power. In this case, the power balance is maintained. However, in the case of more PV sources, the situation is more complex. Using the information about the power balance occurring in the microgrid, loads might be controlled to reach the power balance still before reclosing. Consequently, the nominal values of frequency and voltage were reached almost immediately after the supply restoration.

VI. CONCLUSION

The Vector Shift criterion was utilized only in power system protection devices. The application of this algorithm covered mainly island detection. However, the Vector Shift criterion has become increasingly unpopular in the last few years. The reason is related to unfavorable, false tripping, which caused shutdowns of distributed generation. Depending on the power of a generating unit, the problem was more or less considerable. In the worst cases, the results could even affect the stability of the power system. These negative features were particularly described in the following article. Comprehensive research was conducted to prove the technical problems accompanying the utilization of the Vector Shift. Eventually, the authors illustrate the reasons for banning this criterion in some countries. However, the authors of this paper also presented the new features and properties of the Vector Shift algorithm. These features could change the application of the Vector Shift from power system protection to the regulatory processes of distributed energy sources. Therefore, the Vector Shift criterion could be utilized in modern grids and microgrids. Furthermore, potential applications have also been proposed in the article. These applications might improve the operation of distributed generation and allow the effective utilization of green energy. Moreover, in the era of digitalization, these ideas can be successfully applied to Smart Grids. As a final point, the authors would like to invite other scientists to discuss, and research related to this topic.

REFERENCES

[1] D. Tzelepis, A. Dysko, and C. Booth, "Performance of loss-of-mains detection in multi-generator power islands," in *Proc. 13th Int. Conf. Develop. Power Syst. Protection (DPSP)*, 2016, pp. 2–7, doi: 10.1049/cp.2016.0066.

[2] G. Heggie and H. T. Yip, "A multi-function relay for loss of mains protection," in *Proc. IEE Colloq. Syst. Implications Embedded Gener. Protection Control*, 1998, p. 5.

[3] O. N. Faqhruldin, E. F. El-Saadany, and H. H. Zeineldin, "Evaluation of islanding detection techniques for inverter-based distributed generation," in *Proc. IEEE Power Energy Soc. Gen. Meeting*, Jul. 2012, pp. 1–7, doi: 10.1109/PESGM.2012.6345001.

[4] J. Xavier, "Protection & control strategy for effectively interconnecting and islanding distributed energy resources during grid disturbances," in *Proc. 72nd Conf. Protective Relay Eng. (CPRE)*, Mar. 2019, pp. 1–10, doi: 10.1109/CPRE.2019.8765888.

[5] M. R. Alam, K. M. Muttaqi, and A. Bouzerdoum, "A multifeature-based approach for islanding detection of DG in the subcritical region of vector surge relays," *IEEE Trans. Power Del.*, vol. 29, no. 5, pp. 2349–2358, Oct. 2014, doi: 10.1109/TPWRD.2014.2315839.

[6] A. M. Tayebi and M. Akhbari, "A comparison between frequency relays and vector surge relays for synchronous DG anti-islanding protection," in *Proc. Eurocon*, Jul. 2013, pp. 701–705, doi: 10.1109/EUROCON.2013.6625059.

[7] Z. Matišić, J. Havelka, M. Bolfek, and A. Marušić, "Vector surge and rocof protection algorithms for distributed generator islanding detection," in *Proc. Medit. Conf. Power Gener., Transmiss., Distrib. Energy Convers. (MEDPOWER)*, 2018, pp. 3–8, doi: 10.1049/cp.2018.1918.

[8] R. Bugdal, A. Dysko, G. M. Burt, and J. R. Mcdonald, "Performance analysis of the ROCOF and vector shift methods using a dynamic protection modelling approach," in *Proc. 15th Int. Conf. Power System Protection*, 2006, pp. 139–144.

[9] A. J. Roscoe, G. M. Burt, and C. G. Bright, "Avoiding the non-detection zone of passive loss-of-mains (islanding) relays for synchronous generation by using low bandwidth control loops and controlled reactive power mismatches," *IEEE Trans. Smart Grid*, vol. 5, no. 2, pp. 602–611, Mar. 2014, doi: 10.1109/TSG.2013.2279016.
[10] K. Maki, A. Kulmala, S. Repo, and P. Jarventausta, "Problems related to islanding protection of distributed generation in distribution network," in *Proc. IEEE Lausanne Power Tech.*, Jul. 2007, pp. 467–472, doi: 10.1109/PCT.2007.4538362.
[11] J. C. M. Vieira, D. S. Correa, W. Freitas, and W. Xu, "Performance curves of voltage relays for islanding detection of distributed generators," *IEEE Trans. Power Syst.*, vol. 20, no. 3, pp. 1660–1662, Aug. 2005, doi: 10.1109/TPWRS.2005.852128.
[12] J. C. M. Vieira, S. Member, W. Freitas, W. Xu, and A. Morelato, "Distributed generation protection," *Power*, vol. 21, no. 3, pp. 1120–1127, 2006.
[13] W. Freitas, W. Xu, C. M. Affonso, and Z. Huang, "Comparative analysis between ROCOF and vector surge relays for distributed generation applications," *IEEE Trans. Power Del.*, vol. 20, no. 2, pp. 1315–1324, Apr. 2005, doi: 10.1109/TPWRD.2004.834869.
[14] D. M. Laverty, D. J. Morrow, R. J. Best, and P. A. Crossley, "Differential ROCOF relay for loss-of-mains protection of renewable generation using phasor measurement over internet protocol," in *Proc. CIGRE/PES-Integr. Wide Scale Renew. Resour. Power Del. Syst. Symp.*, Calgary, AB, Canada, 2009.
[15] M. Delfanti, D. Falabretti, M. Merlo, G. Monfredini, and V. Olivieri, "Dispersed generation in MV networks: Performance of anti-islanding protections," in *Proc. 14th Int. Conf. Harmon. Quality Power (ICHQP)*, Sep. 2010, pp. 1–6, doi: 10.1109/ICHQP.2010.5625446.
[16] C. Booth, *Loss of Mains Protection*. Bristol, U.K.: Western Power Distribution, DSOF Jun. 2018, pp. 1–74.
[17] W. Freitas, Z. Huang, and W. Xu, "A practical method for assessing the effectiveness of vector surge relays for distributed generation applications," *IEEE Trans. Power Del.*, vol. 20, no. 1, pp. 57–63, Jan. 2005, doi: 10.1109/TPWRD.2004.838637.
[18] W. Freitas and W. Xu, "False operation of vector surge relays," *IEEE Trans. Power Del.*, vol. 19, no. 1, pp. 436–438, Jan. 2004, doi: 10.1109/TPWRD.2003.820412.
[19] M. H. Hairi and H. Li, "Sensitivity and stability analysis of loss of main protection in active distribution networks," in *Proc. IEEE PES Gen. Meeting | Conf. Expo.*, Jul. 2014, pp. 1–5, doi: 10.1109/PESGM.2014.6939341.
[20] M. Hou, H. Gao, Y. Lu, Y. Zhang, H. Cao, and Y. Lin, "A composite method for islanding detection based on vector shift and frequency variation," in *Proc. Asia–Pacific Power Energy Eng. Conf.*, Mar. 2010, pp. 1–4, doi: 10.1109/APPEEC.2010.5448252.
[21] I. V. Banu, M. Istrate, D. Machidon, and R. Pantelimon, "A study on anti-islanding detection algorithms for grid-tied photovoltaic systems," in *Proc. Int. Conf. Optim. Electr. Electron. Equip. (OPTIM)*, May 2014, pp. 655–660, doi: 10.1109/OPTIM.2014.6850940.
[22] M. R. Alam, M. T. A. Begum, and K. M. Muttaqi, "Assessing the performance of ROCOF relay for anti-islanding protection of distributed generation under subcritical region of power imbalance," *IEEE Trans. Ind. Appl.*, vol. 55, no. 5, pp. 5395–5405, Sep./Oct. 2019, doi: 10.1109/TIA.2019.2927667.
[23] T. Bašakarad, N. Holjevac, I. Kuzle, I. Ivanković, and N. Zovko, "ROCOF importance in electric power systems with high renewables share: A simulation case for Croatia," in *Proc. 12th Medit. Conf. Power Gener., Transmiss., Distrib. Energy Convers. (MEDPOWER)*, 2021, pp. 72–77, doi: 10.1049/icp.2021.1239.
[24] J. A. Barrios-Gomez, F. Sanchez, G. Claudio, F. Gonzalez-Longatt, M. Acosta, and D. Topic, "RoCoF calculation using low-cost hardware in the loop: Multi-area Nordic power system," in *Proc. Int. Conf. Smart Syst. Technol. (SST)*, Oct. 2020, pp. 187–192, doi: 10.1109/SST49455.2020.9264119.
[25] M. O'Donovan, E. O'Callaghan, N. Barry, and J. Connell, "Implications for the rate of change of frequency on an isolated power system," in *Proc. 54th Int. Universities Power Eng. Conf. (UPEC)*, Sep. 2019, pp. 1–5, doi: 10.1109/UPEC.2019.8893446.
[26] P. Wright and G. Rietveld, "Standard tests and requirements for rate-of-change of frequency (ROCOF) measurements in smart grids," Nat. Phys. Lab. Webinar, May 2019. [Online]. Available: https://www.rocofmetrology.eu
[27] F. Gonzalez-Longatt, J. M. Roldan-Fernandez, H. R. Chamorro, S. Arnaltes, and J. L. Rodriguez-Amenedo, "Investigation of inertia response and rate of change of frequency in low rotational inertial scenario of synchronous dominated system," *Electronics*, vol. 10, no. 18, p. 2288, Sep. 2021, doi: 10.3390/electronics10182288.
[28] J. Machowski, Z. Lubosny, J. W. Bialek, and J. R. Bumby, *Power System Dynamics: Stability and Control*, 3rd ed. Hoboken, NJ, USA: Wiley, Feb. 2020, p. 888.
[29] A. Vukojevic and S. Lukic, "Microgrid protection and control schemes for seamless transition to island and grid synchronization," *IEEE Trans. Smart Grid*, vol. 11, no. 4, pp. 2845–2855, Jul. 2020, doi: 10.1109/TSG.2020.2975850.
[30] I. Kim and R. G. Harley, "A study on the intentional island formed by the residential photovoltaic system and the challenges to island operation," in *Proc. North Amer. Power Symp. (NAPS)*, Oct. 2015, pp. 5–9, doi: 10.1109/NAPS.2015.7335205.

KAROL SWIERCZYNSKI received the M.Sc. degree from the Faculty of Electrical Engineering, Wroclaw University of Science and Technology, in 2019, where he is currently pursuing the Ph.D. degree with the Doctoral School. He has combined professional work in the power industry with doctoral studies for versatile self-development. Currently, he is developing new protection criteria to improve the operation of distributed energy resources in microgrids. His research interests include power system protection, especially in medium-voltage grids.

MARCIN HABRYCH received the M.Sc. and Ph.D. degrees from the Institute of Electrical Power Engineering, Wroclaw University of Science and Technology, in 2002 and 2007, respectively, and the D.Sc. degree. Since 2008, he has been an Assistant Professor with the Wroclaw University of Science and Technology. As a D.Sc. student, he has focused on the subject of power system protection, power line communications, current and voltage converters, and reactive power compensation.

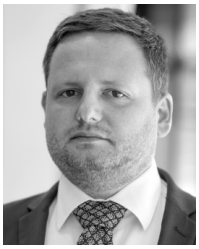

BARTOSZ BRUSILOWICZ (Senior Member, IEEE) was born in Wroclaw, Poland, in 1984. He received the M.Sc. and Ph.D. degrees in electrical engineering from the Wroclaw University of Science and Technology (WUST), in 2009 and 2013, respectively. He is an Assistant Professor with the Department of Electrical Power Engineering, WUST. From February 2018 to February 2019, he was a Visiting Professor with Washington State University, Pullman, USA. Since October 2022, he has been a Postdoctoral Fellow with the University of Idaho, Moscow, USA. His research interests include voltage stability, power system protection, and digital signal processing.